

## Fatigue Failure of Alloy Grade P22 Hot Reheat Auxiliary Steam Pipe

Anis Muneerah Shaiful Bahari<sup>1</sup>, Saidatul Akmal Biyamin<sup>1\*\*</sup>, Muhammad Hilmi Khairuddin<sup>2</sup>, Ng Guat Peng<sup>1</sup>, Norlia Berahim<sup>2</sup>, Saiful Adilin Shokri<sup>1</sup>, Mohd Hafiz Abdul Ghaffar<sup>1</sup>, Mazmi Yahya<sup>1</sup>, Robiah Ghazali<sup>1</sup>

<sup>1</sup>Materials Engineering & Testing Group, Tenaga Nasional Berhad Research Sdn. Bhd., 43000 Kajang, Selangor, Malaysia.

<sup>2</sup>Plant Inspection Services, Tenaga Nasional Berhad Research Sdn. Bhd., 43000 Kajang, Selangor, Malaysia.

Received 11 January 2023, Revised 5 May 2023, Accepted 15 May 2023

### ABSTRACT

*A leak was discovered in the hot reheat auxiliary pipe. The pipe was found to have a bulging condition and a crack at the base metal area. A circumferential crack was discovered near a repair weld spot on the external surface. The failure was investigated using material characterization techniques, including in-situ replication, glow discharge spectroscopy (GDS), microhardness analysis, optical microscopy, and energy dispersive X-ray spectroscopy (EDX). Based on microstructure analysis, numerous cracks were observed to have initiated at the internal surfaces of the pipe. Most of the cracks were found on the parent metal. The cluster of cracks concentrates on the plane of  $0^{\circ}$  -  $180^{\circ}$ . Microstructure analysis shows that the cracks are multiple, parallel, mainly transgranular, oxide-filled with branching crack tips. It is thought that the cracking is associated with fatigue and, most likely, high cyclic stress is the key contributory factor. The steam oxide cracked gradually as a result of the cyclic stress. As more metal surface was exposed, new oxide formed, causing cracks to propagate into the metal as this process was repeated due to cyclic loading.*

**Keywords:** Cracking filled oxide, cyclic stress, fatigue.

## 1. INTRODUCTION

An increasing number of underground pipelines have been built to transport oil and natural gas resources as the demand for these commodities has grown quickly [1]. However, pipeline leakage accidents regularly happen, resulting in major social repercussions and financial losses [2]. One of the biggest risks to the integrity and longevity of pipelines is corrosion damage [3]; between 30% and 50% of oil and/or gas pipeline failures have been linked to corrosion. Besides that, fatigue loading is also one of the main causes of pipe component failures [4]. Even under typical operating circumstances, premature failures may take place below permissible stress limits. This can be attributed to the pre-existing defects or cracks that are not detected during the pre-service inspection or operation fault that leads to premature cracking as the component was exposed and degraded over time.

A phenomenon known as fatigue cracking is brought on by the fundamental characteristics of fracture mechanics. Defects like fracture displacement may arise when the tension on a structure exceeds its tensile strength, a process that may progress over time [5]. The term "fatigue" is employed because the cyclical and repetitive stress causes the material to appear "weary". A cylindrical body, like a pipe, may have cracks running along it or all the way around it. An axial crack is a crack that moves axially across a pipe. A circumferential crack moves around the circle of a pipe. In this case, a circumferential crack was reported in the auxiliary

---

\* Corresponding author: saidatul.biyamin@tnb.com.my

steam pipe [5]. In this study, the characteristics and causes of failure of the aforementioned pipeline were analysed. This case study is crucial to improving knowledge of auxiliary pipe failure. This study will explain everything in detail with good visuals. The investigation of pipe hangers and supports was also elaborated.

## 2. MATERIAL AND METHODS

### 2.1 Materials

The material is a hot reheat auxiliary steam pipe that experienced leakage. The pipe has been operating for more than 130,000 equivalent operating hours (EOH) in a cyclic-load operating power plant. The operating temperature and the operating pressure were 540 °C and 49 bar, respectively. Figure 1 a) depicts the failure of the auxiliary pipe components, which include the pipe spool, reducer, and T-joint. The through-wall crack was identified in the spool pipe. The pipe was found to have bulging and cracks at the base metal area. Multiple linear indications were found at the base metal near the weldment of the spool and reducer. The main crack occurred in the spool over an arch length of 0° to 90°, as shown in Figure 1 b). Figure 1 c) shows the as-received spool sample and Figure 1 d) shows the 0° to 180° side of the sectioned pipe with a circumferential main crack through (leakage) as well as multiple fine cracks on the internal surface.

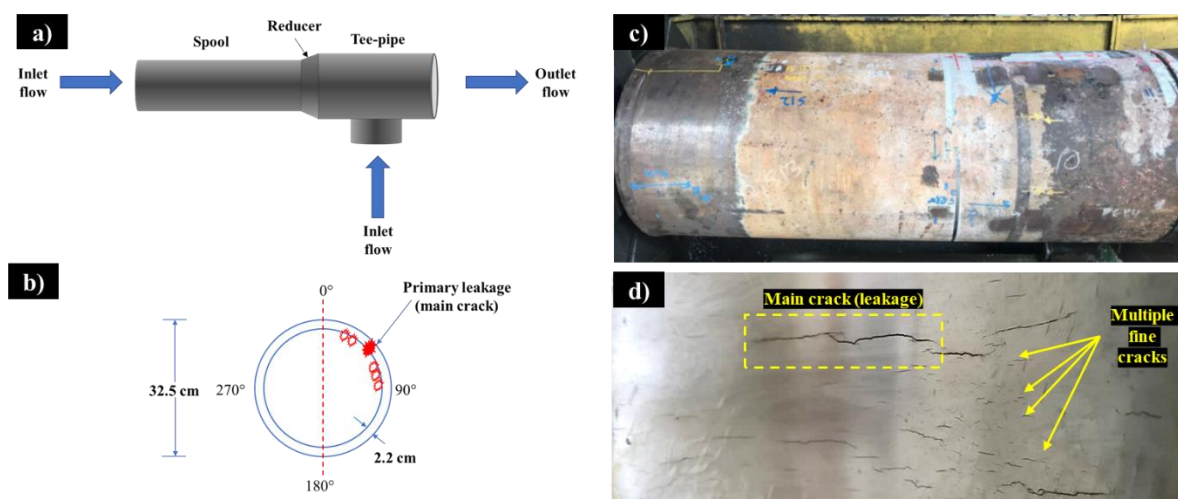


**Figure 1.** a) General illustration of the spool, reducer and tee-pipe b) cross-sectional view of finding on spool c) as-received spool and d) 0° to 180° side of the internal sectioned pipe with the presence of numerous circumferential cracks.

### 2.2 Analysis

According to the specification in Table 1, the steel is low-carbon steel ASTM A335 P22. The Glow Discharge Spectrometer (Spectrums-GDA 750) was used to check compliance with standard chemical composition. Light microscope (Carl Zeiss Axio Imager 2) and Field Emission Scanning Electron Microscopy (FESEM Hitachi SU8020) together with EDX (Bruker XFlash 6/60 detector) were used to study the microstructure of the failed samples. The surface deposit was also collected before the surface was ground to analyze the elemental composition of the deposit.

For microstructure analysis, before the sample in Figure 1 d) was cut, in situ replication was carried out using nital etchants on the unaffected area (at plane of 270°), main crack tip (crack through leakage), and several fine cracks [6]. Then, the samples were cut and mounted using the cold mounting process in hardened resin. The microstructure of the mounted metal surfaces

was prepared using grinding, polishing, and lastly etched with 3% nital (immersed for 5 to 7 seconds) [7]. The Vickers hardness test instrument (Future-Tech, FM1) was used to measure microhardness values in accordance to ASTM E384-2017 [8]. The applied stress was 300 gf, and the average readings from eight indentations per sample were recorded. Additionally, pipe hanger and support visual inspection was conducted during hot conditions in order to inspect the physical condition of nearby pipe hanger readings and the presence of physical damage, if any.

**Table 1** The material composition of standard and failed samples of ASTM A335 P22

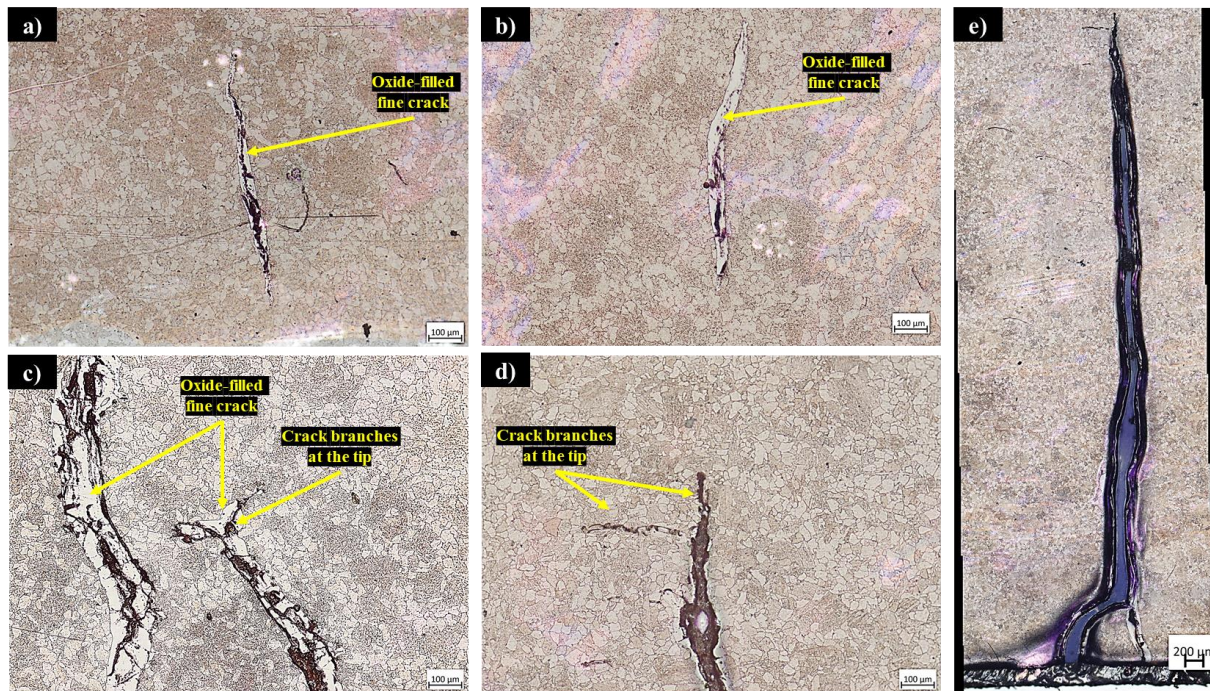
Elements	Fe	C	Mn	Si	P	Cr	Ni
<b>Standard</b>	Bal.	0.05-0.15	0.30-0.60	Max 0.50	Max 0.025	1.9-2.6	-
<b>Fractured</b>	96.168	0.101	0.505	0.241	0.0122	1.939	0.038
Elements	Ti	Cu	Mo	Co	V	Al	Nb
<b>Standard</b>	-	-	0.87-1.13	-	-	-	-
<b>Fractured</b>	-	0.045	0.931	-	-	0.018	0.001

### 3. RESULTS AND DISCUSSION

#### 3.1 Microstructural Analysis

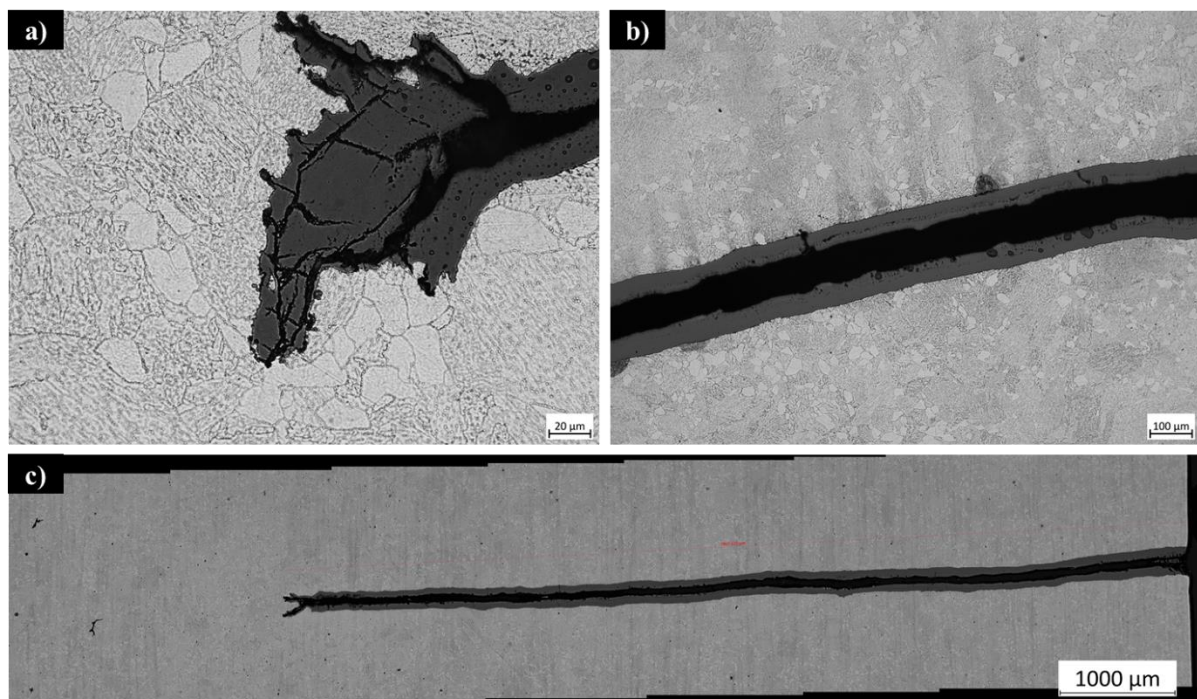
Figure 2 shows the microstructures of in-situ replication for P22 alloy etched with nital. All the microstructures show that the cracks occurred at the base metal. Figure 2 a) shows the unaffected area microstructure at the plane of 270° which consists of ferrite and bainite phases. Based on the thermal degradation classes as given by the Central Electricity Generating Board (CEGB), it shows that the microstructure of the as-received spool has degraded with bainite decomposition to class B, in which the carbides have spheroidized in a moderate manner, as compared to the new microstructure of tempered bainitic steel [9] which has well-defined bainite colonies. Figure 2 a) shows that the bainite phase has started to break up and the presence of carbides is observed in the base metal. Figure 2 b) and Figure 2 c) show fine cracks filled with oxide. Figure 2 c) and Figure 2 d) show the split at the crack tips of the main crack and fine crack, respectively. Figure 2 e) shows a sharp, straight primary crack. The main characteristic of the fine cracks associates with propagation in a transgranular mode and oxide-filled. Such a crack appearance is associated with fatigue [10].

Figure 3 shows the microstructures of the mounted sample etched using nital. All the mounted samples show parallel cracks on the surface of the spool. The characteristics of the cracks are similar to those shown in replica films, which are multiple, parallel fine cracks that are propagated in transgranular mode and filled with oxide. Figure 3 a) shows the crack tip with small branches at the end, and Figure 3 b) shows the thick oxide layer in the crack. Most of the cracks are filled with oxides, which form at high temperatures and crack or rupture during operation cycles. The oxide layer filling the cracks is a mixture of dense and cracking/exfoliated layers due to its brittle characteristic.



**Figure 2.** Microstructure of in-situ replication P22 alloy etched with nital revealing a) unaffected base metal at the plane of 270° (magnification at 100X) b) fine crack (magnification at 100X) c) fine crack (magnification at 100X) d) crack tip of the main crack (magnification at 100X) e) crack tip (magnification at 50X)

Figure 3 c) shows the microstructure of the mounted transverse sample to show the crack depth. The crack was measured using ZEN Core 3.3. The crack shows a transgranular sharp crack with oxide filled and split ends. The deepest crack has already penetrated up to approximately 7.9 mm.



**Figure 3.** Microstructure of mounted P22 alloy etched with nital revealing a) oxide filled fine crack with branching tip (magnification at 500X) b) heavily oxidized cracking surface (magnification at 100X) c) crack depth (magnification at 50X)

### 3.2 Elemental Analysis

Figures 4 a), b) and c) show the EDX analysis of the oxide deposit, white phase at the crack, and base metal near the crack, respectively. Oxide deposits were collected at the internal surface using carbon tape. Figure 4 a) shows a high oxygen content (30.81%) in the deposits at the internal surface, which suggests the presence of oxide at the internal surface of the spool. Besides that, Figure 4 b) shows the EDX analysis of the unknown white phase. The result of oxygen content is quite high (similar to an oxide deposit), which suggests the white phase shown on the replica film, is the formation of oxide in the base metal. Figure 4 c) shows the EDX analysis of the base metal near the crack. The result of oxygen is relatively low, which is consistent with the chemical composition result of P22 alloy.

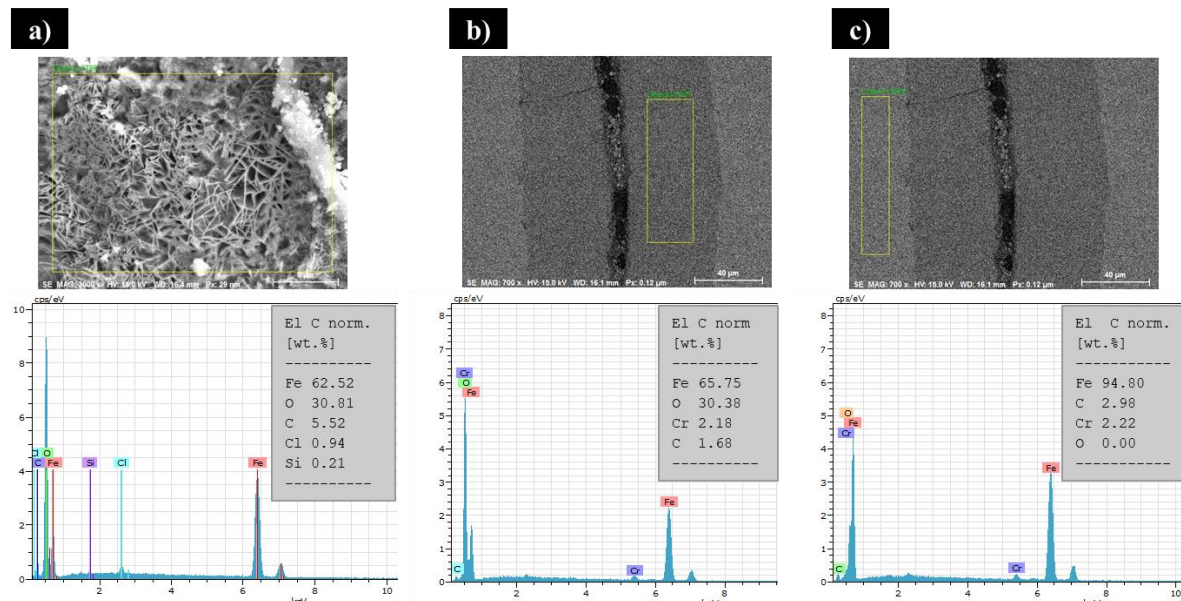


**Figure 4.** Multipoint EDX analysis of a) deposit at the internal surface b) white phase c) base metal.

In addition, EDX analysis using the line profile scanning method was done to confirm the elemental composition of the crack as shown in Figure 5. The elements that were observed were oxygen (O), iron (Fe) and chromium (Cr). It shows that oxygen content rises rapidly at the unknown phase, which clarifies the phases as oxide. It was revealed that the oxide layer is mostly composed of magnetite ( $Me_3O_4$ ), when Me stands for metal such as Mo, Cr and Fe [5]. No apparent corrosive elements and no significant corrosion pits were found.

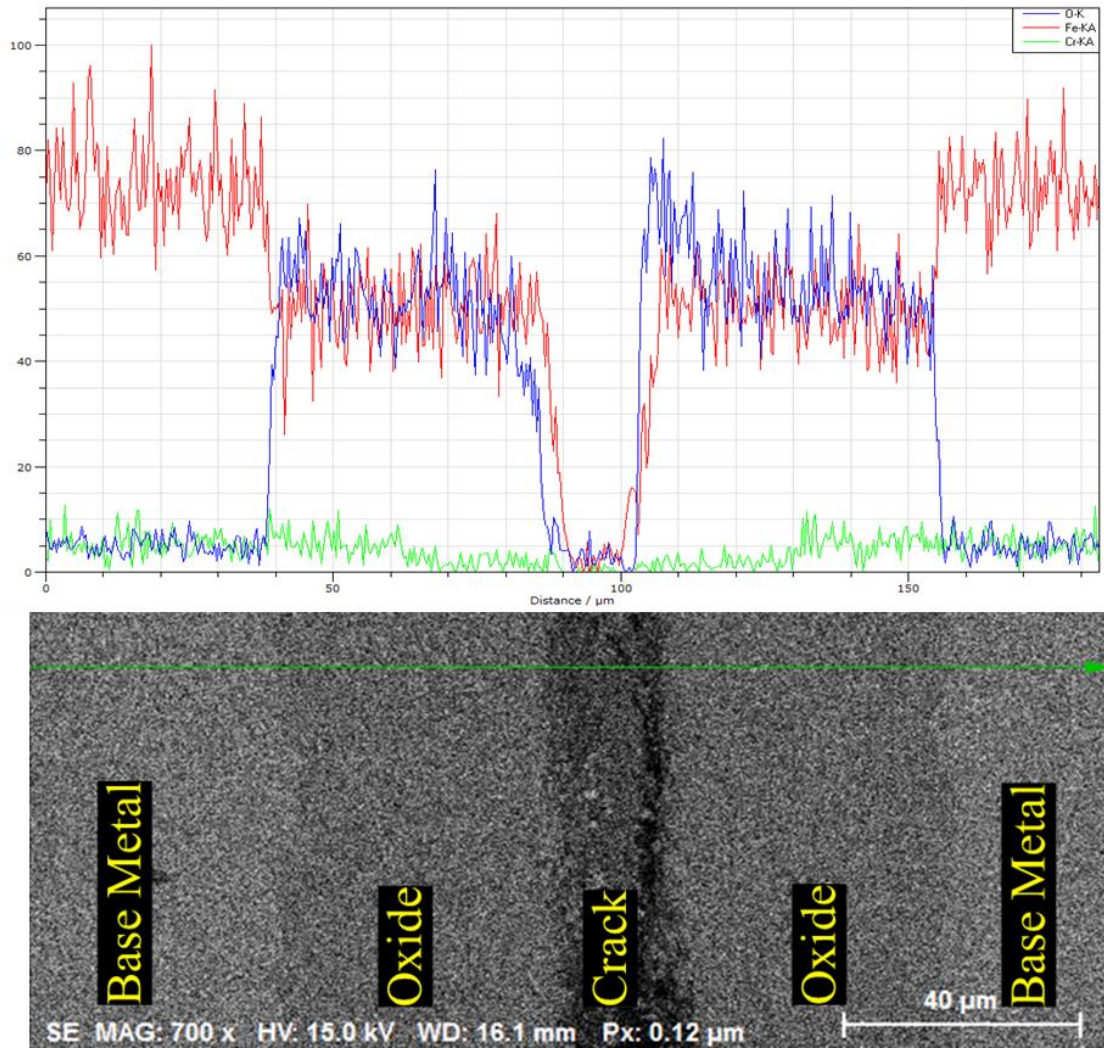


**Figure 5.** EDX profile scanning analysis relative to the region shown in the SEM.

### 3.3 Microhardness Testing

The microhardness testing was done at different locations, which are near the crack and unaffected area. The microhardness values near the crack were in a range of 148 HV to 155 HV, whereas the unaffected area's hardness values were in a range of 147 HV to 156 HV. The hardness values at the near crack and unaffected areas are within the acceptable range of standard P22 materials as the maximum allowable hardness for P22 is 170 HV [11]. Based on these results, it shows that the steel exhibited normal hardness properties which suggests that the failure is not associated with embrittlement or softening issue in steels.

### 3.4 Pipe Hanger and Support Inspection

Additional information on pipe hanger inspection was obtained to identify the possible root cause of failure. It was reported that there are three hangers, which are H1 (constant hanger), H2 (rigid support) and H3 (variable hanger) in the neighbourhood of the pipe leakage as illustrated in Figure 6.

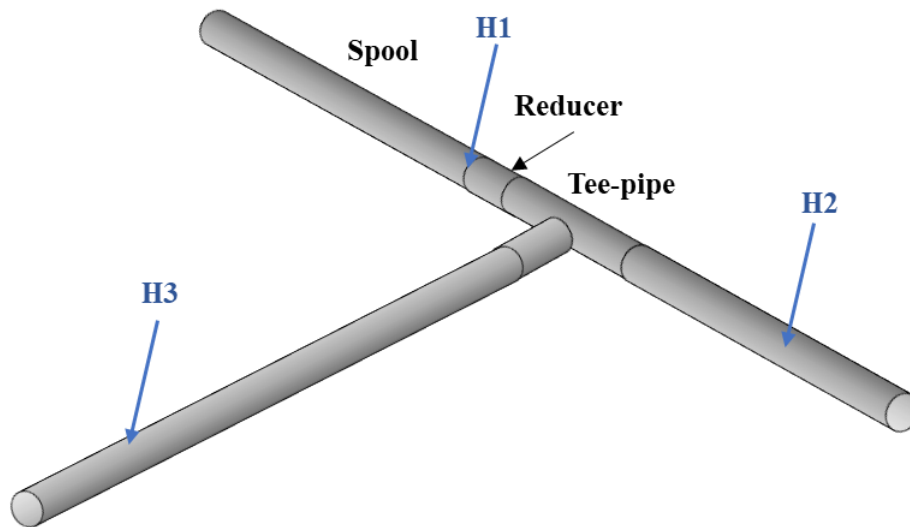


**Figure 6.** General illustration of nearby hanger location at hot reheat auxiliary pipe.

The inspection shows that H2 and H3 were still within the allowable range. H1, however, was reported in bottom over-scaled condition. A pipe hanger that is bottom over-scaled acts like a rigid hanger because it is unable to accommodate the pipe's thermal movement. The movement is constrained, and the pipe may experience increased stress as a result [12]. This suggests that the hanger is overloaded at that particular location where the hanger's suspended beam was found deformed. The malfunctioning pipe hanger could cause load transfer to adjacent piping sections [12] and introduce high-stress locations.

Besides, it was observed that some pipe snubbers of Hot Reheat Pipe (HRP) that connected close to auxiliary pipes showed signs of hydraulic fluid leakage, and fluid indicator showed low level or below minimum level or exhausted oil. As the snubbers hydraulic fluid was exhausted, it will not be functioning correctly. This condition is aggravated when air or dirt enters the snubber's valve. The snubber is used to protect the piping system from shock/transient load. When the snubber is not functioning correctly, it could not resist and protect the piping system from transient (as snubber freely slides; thus, it does not counteract the shock forces) [12]. Furthermore, broken pipe support strut ends, dislodged snubber pins and dislodged snubber ends were found on the HRP line show the sign of pipe snubbers have started to become malfunction. Based on the pipe hanger and support condition, it shows that the crack is likely attributed to the excessive cyclic stress on the piping system [12].

### 3.5 Possible Mechanisms

The failure mechanism reported in several studies was summarized as having three main possible factors. The first is the possible cracking of the oxide layer as a result of differences in thermal expansion coefficients between the pipe material and the oxide during start-stop cycles [5]. Second, the fatigue cracks caused by sway movement fluctuations or rigid fixing of assemblies during operation [5,12]. This is related to the faulty pipe hanger near the spool that has become overscaled, as discussed in the previous section. Lastly, a high thermal stress due to cyclic loading or pressure change during load swing [10,12]. The cyclic stress caused steam oxide to crack in a progressive manner, driving crack propagation into metal.

According to the characteristics of the cracks in this study, the failure mechanism was probably associated with thermal fatigue or corrosion fatigue. However, the EDX results did not show

apparent corrosive elements and no significant corrosion pits were found, it was deduced that the main driving factor is thermal fatigue.

#### 4. CONCLUSION

The cracks that occur on the base metal are initiated from the internal surface. The cracking region was found on the 0°-180° plane. Based on microstructure analysis, numerous parallel cracks were primarily transgranular, oxide-filled, with branching crack tips. The above characteristics suggest that the cracking is associated with fatigue and most likely, high cyclic stress is the key contributory factor. The cyclic stress caused the steam oxide to crack in a progressive manner; new oxide formed as more underneath metal was exposed, driving the cracks to propagate into metal. The high cyclic stress is probably a contributing factor to the presence of high bending stress on the pipe. This may be caused by the faulty pipe hangers that have been experiencing over-scaling conditions in a short period despite the adjustment and abnormal pipe movement due to cyclic thermal loading, water hammer, malfunctioning of valves etc. The heavily oxidized cracking surfaces suggest that the cracks had existed for a long period. The fatigue mechanism is a time-dependent process. The cracks may take months or years to fully penetrate the pipe wall to form a leak, depending on the operation cycles & driving factors.

#### ACKNOWLEDGEMENTS

The authors would like to acknowledge the support of management team from TNB Power Generation & TNB Research Sdn Bhd.

#### REFERENCES

- [1] J. L. Pacheco, W. J. Sisak, S. Venaik, R. V. Reddy, D. R. Robson, A. Dhokte, E. J. Wright, D. Pugh, C. E. Curtis and S. R. Hickman, "Advances in Wet Gas Pipeline Technology," in Proc. International Petroleum Technology Conference, Dubai, (2007) no. 11382.
- [2] M. C. Li, Y. F. Cheng, *Electrochem. Acta*, vol **53**, issue 6 (2008) pp. 2831-2836.
- [3] X. G. Li, D. W. Zhang, Z. Y. Liu, *Nature*, vol **527** (2015) pp. 441-442.
- [4] P. Arora, P. K. Singh, V. Bhasin, K. K. Vaze, D. M. Pukazhendhi, P. Gandi, G. Raghava, "Fatigue crack growth behavior in Pipes and Elbows of Carbon Steel and Stainless Steel Materials," in Proc. 6th International Conference on Creep, Fatigue and Creep-Fatigue, (2013) pp. 703-709.
- [5] B. Erenburg, A. Zilberberg, E. Iskevitch, *J. Fail. Anal. and Preven.* vol **19**, issue 2 (2019) pp. 320-327.
- [6] VGB Standard, VGB PowerTech Service GmbH, Essen, (2014).
- [7] Standard Practice for Microetching Metals and Alloys, ASTM International, (2015).
- [8] ASTM E384 Knoop and Vickers Hardness Testing, ASTM International, (2017).
- [9] T. Salonen P. Auerkari, *Espoo*, issue 280 (1996).
- [10] Guidelines for the Nondestructive Examination of Boilers, EPRI, California, (2007).
- [11] Maximum Allowable Stress Values S for Ferrous Materials according to ASME Code Section II, ASME International, (2021) 6-161.
- [12] H. Rezaei, B. Ryan, I. Stoianov, "Pipe Failure Analysis and Impact of Dynamic Hydraulic Condition in Water Supply Networks," in Proc. 3th Computer Control for Water Industry Conference(CCWI), (2015) pp. 253-262.